

1 **Factors influencing the estimation of aboveground biomass (AGB) in tropical forests using**
2 **RADAR remote sensing.**

3 Victoria E. Espinoza-Mendoza^{1,2*}

4 ¹Departamento de Ecología y Ciencias Ambientales (DECA – CEBBAD) Universidad
5 Maimónides. Buenos Aires, Argentina; ²Consejo Nacional de Investigaciones Científicas y
6 Técnicas (CONICET). Buenos Aires, Argentina.

7 *correo electrónico: espinoza.victoria@maimonides.edu

8

9 **Abstract**

10 Despite the large amount of accessible spatial information, the issue of estimating aboveground
11 biomass through remote sensing, especially radar, remains a challenge in complex ecosystems
12 such as tropical forests. One of the advantages of radar sensors is that of "crossing clouds"
13 (capacity that does not have optical images like Landsat), facilitating their use in areas with
14 permanent cloud cover. This work defines, from several studies conducted in tropical forests
15 using ALOS PALSAR, which are the factors with the most influence on the signal of the radar.
16 This can be useful in the development and/or improvement of methodologies to estimate
17 aboveground biomass in tropical forests, combining field data and satellite imagery of radar.

18

19 **Keywords: biomass, radar, ALOS PALSAR, remote sensing, L-band.**

20

21

22

23

24

25 **Introduction**

26 In recent years, the estimation of aboveground biomass (AGB) through the combination of field
27 data and remote sensing has been gaining ground, because it becomes an option that reduces
28 costs, in addition to obtaining information in areas of difficult access (Koch 2013).

29 Biomass is the total amount of plant material present in a specific area (Drake et al., 2003). The
30 aerial component of the arboreal stratum represents one of the main stores of biomass and carbon
31 (Quijano & Morales 2016). There are several methods to estimate AGB, being classified as
32 destructive or direct (cut, dry and weigh the tree) and non-destructive or indirect (allometric
33 equations) (Sola et al., 2012, Walker 2011). Allometric equations usually include three variables:
34 diameter at breast height (DBH), tree height and wood density; through which we can obtain the
35 ABG in the field.

36 The estimation of AGB using remote sensing remains a challenge, especially in such complex
37 ecosystems as tropical forests (Hamdan et al., 2014b). Research conducted by Avitabile et al.
38 (2015), Baccini et al. (2012), Goetz et al. (2009) and Mitchard et al. (2013) using optical and / or
39 radar images show different methods used for the estimation of AGB and carbon stocks by
40 remote sensing in tropical forests around the world. They emphasize the ability of radar satellite
41 images such as ALOS PALSAR to "pass through the clouds" (capacity with which optical images
42 do not count as LANDSAT), this feature being very useful in tropical areas with permanent cloud
43 cover.

44 Although there is little information available that indicates exactly what climatic or biophysical
45 factors affect the estimation of AGB in tropical forests at local scales; Studies such as those by
46 Hamdan et al. (2014b), Sinha et al. (2015) and Espinoza-Mendoza (2016) provide valuable

47 information. Hamdan et al. (2014b) found in Malaysia, that the allometric equations have a great
48 influence on the response of the sensor when estimating biomass. In addition, the size of the trees
49 and the diametric groups also influenced the estimated biomass values by means of radar images.
50 On the other hand, Espinoza-Mendoza (2016), found in the forest of Nicaragua, that the number
51 of trees per hectare is a very important factor when correlating the backscattered value of the
52 radar with the biomass estimated in the field.

53 The present work aims to define, based on various studies in tropical forests, which factors are
54 those that would have a greater influence when estimating biomass by radar images (especially
55 ALOS PALSAR). It should be noted that in this research, factors referring to technical and
56 structural aspects of the forest are mentioned, focusing more on the latter. Knowing these factors
57 and the level of influence that hold, would be of great support in the development and / or
58 improvement of methodologies for estimating ABG in tropical forests combining field data and
59 remote sensing.

60

61 **Technical aspects of radar images: wavelength and polarization**

62 The frequency of the SAR radar is directly proportional to the depth of penetration of the wave,
63 meaning that short waves can only penetrate the forest by a few centimeters while long waves
64 can interact with the forest floor (Imhoff 1995). The L band is the least influenced by the
65 environmental conditions, therefore, it obtains better information of the structural components of
66 the forest by having a better interaction with the trunk and the branches, being the most adequate
67 for estimating biomass (Ghasemi et al. 2011, Joshi et al 2015b, Luckman et al 1997, Yu and
68 Saatchi 2016).

69 In the same way, the P band has a good correspondence with the biomass. Both long wavelengths
70 can penetrate the canopy, dispersing the energy towards the woody components, being related to
71 biophysical parameters of the trees (Sinha et al 2015, Yu and Saatchi 2016). On the other hand,
72 the X band, is dispersed by the leaves and surface of the canopy, which is feasible to obtain
73 access to the information of the upper layers of the trees. While the C band penetrates through the
74 leaves being dispersed by small branches and elements of the intermediate canopy (Ghasemi et
75 al., 2011). The signal of this last length, although it is true to some extent extends beyond the
76 canopy, becomes attenuated when into contact with more closed canopies and with more
77 structural components, so it works best only in coverage with low amount of biomass (Ghasemi
78 et al., 2011), being less sensitive to the increase in forest volume than the L band (Puliainen et al.,
79 1999).

80 On the other hand, the polarization of the signal is related to the direction of the electric field of
81 the electromagnetic waves and depends on the interaction between the signals emitted and the
82 reflective elements (Sinha et al., 2015). The radar signals are emitted in four polarization
83 combinations: horizontal (HH), vertical (VV) or crossed (HV, VH) (Ghasemi et al., 2011). All
84 these types of polarization will be influenced by the vertical and / or horizontal structure of the
85 forests; so they will interact with different orientations and structures of their components.

86 Several studies have shown the superiority of HV polarization over HH polarization, indicating
87 that HV has a greater sensitivity with biomass, being less influenced by soil moisture and
88 vegetation (Behera et al., 2016, Collins et al., 2009). Hamdan et al 2011, Michelakis et al 2015,
89 Sandberg et al 2011, Van Zyl 1993). On the contrary, studies such as those of Wang et al. (1995)
90 indicate that HH polarization can provide a good means of estimating biomass in coniferous
91 forest. This polarization interacts in a better way with the trunk and biomass of the canopy
92 (Beaudoin et al., 1994), presenting a direct surface-trunk relationship (Wang et al., 1995).

93 Finally, we consider that bands of long lengths such as L or P, with cross polarizations such as
94 HV or VH, give better results than short wave bands such as C or X with simple polarizations HH
95 or VV (Dobson et al., 1992; Le Toan et al. 1992).

96

97

98

99 **Alometry**

100 Allometry is one of the factors related to the most important forest parameters to be considered,
101 probably well above the elaboration of the biomass model. The use of allometric equations that
102 consider three basic parameters: diameter at breast height (DBH), tree height and wood density of
103 the species, can give us more accurate estimates.

104 In some cases, the presence of biases is unavoidable due to inaccuracies on measurement
105 parameters on the field, we must consider evaluating the use of each of them (Keller et al., 2001,
106 Ketterings et al., 2001). Whereby, it is key to consider the methodology used for its calculation. If
107 we do not know the methodology, we doubt about this or observe data inconsistencies, such as
108 the lack of use of specialized instruments to measure heights; we recommended use equations
109 that only consider DBH, since our results could be over or underestimating the AGB and
110 therefore the model results.

111 We will consider that the use of local allometric equations for a particular type of forest or
112 species can give us a more accurate estimate. But if this were not the case, generic equations like
113 Chave et al. (2014b), Brown (1997) updated by Pearson et al. (2005), Feldpausch et al. (2006),
114 among others, provide excellent estimates considering the indicated parameters (Table 1).

115 For example, Hamdan et al. (2014a) used five allometric equations, determining that the best
116 correlation with the radar signal was the allometric equation of Kato et al. (1978). While
117 Espinoza-Mendoza (2016) worked with Brown's equations (1997) updated by Pearson et al.
118 (2005) developed for tropical forests and Chave et al. (2001); both equations only consider the
119 DBH parameter. In the case of Espinoza-Mendoza (2016) no significant statistical differences
120 were found between both equations, so it was decided to use the Brown equation (1997) updated
121 by Pearson et al. (2005).

122
123 **Aspects of the forest structure: density, heterogeneity, diameter groups and**
124 **types of dispersion in forests.**

125 There are studies using remote radar sensors that have estimated biomass in tropical forests. Most
126 of these have been carried out in coniferous forests and pine savannas, justifying that the sensor
127 cannot be used in dense tropical forests or in forests with biomass greater than 100 Mg ha⁻¹
128 (Mermoz et al., 2014b; Mitchard et al., 2009; Woodhouse et al., 2012). Therefore, it is considered
129 that the density and structural complexity of some forest types can have a great influence on the L
130 band of ALOS PALSAR (Michelakis et al., 2015). The work carried out by Espinoza-Mendoza
131 (2016), pioneer in Nicaragua, and one of the first in Central America to discuss the role of the
132 factors that impact on the estimation of biomass with radar in broadleaf and coniferous forests,
133 found a big difference in correlating both types of forest with the radar signal. The study showed
134 that the coniferous forest correlated quite well ($n = 40$, $r_p = 0.64$, $pvalue < 0.0001$), while the
135 broadleaf forest obtained a low correlation, which only improved when considering > 80 ind per
136 plot of 0.5ha (160 ind / ha) ($n = 34$, $r_p = 0.60$, $pvalue < 0.0002$).

137 Observing these results, we consider that the structure of both forests would be one of the causes.
138 This can be supported by Michelakis et al. (2015) who mention that, sometimes, the weak
139 relationships between the backscatter coefficient and biomass are due to the structural variation
140 of the canopy and the number of trees present in the plots. Therefore, we will discuss the
141 behavior of the radar signal separately for coniferous forests and broadleaf forests.

142 A coniferous forest is structurally less complex than a broadleaved forest (Figure 2). The areas
143 where these forests are located are more open, with low canopy cover and the presence of
144 clearings and/or gaps in the terrain. Therefore, at lower complexity, the radar signal should be
145 dispersed more homogeneously without the influence of a variety of dispersing elements.

146
147 We can consider that, in a coniferous forest, the type of dominant dispersion would be double
148 bounce (Figure 4), because, when there is exposed soil, the signal is emitted towards the ground,
149 bounces off the trunk and then disperses towards the radar, improving the sensitivity of this
150 (Hensley et al., 2014). In addition, in some areas, coniferous forests are not very dense, so the L
151 band would have a positive contribution (Yu and Saatchi 2016).

152 Wang et al. (1995) indicate that the largest amount of biomass of a conifer tree is stored in its
153 trunk. So, it can indeed that to exists double bounce dispersion with surface-trunk interaction, the
154 radar signal would be collecting direct information of the component with higher biomass
155 (trunk). On the other hand, the volumetric dispersion (Figure 4) in this type of forest is very
156 small, which would not contribute significantly in the results of the correlation.

157 The homogeneity present in coniferous forests is not a main feature of a tropical broadleaved
158 forest, since in this last case exists a diversity of species, considered as heterogeneous forests
159 (Figure 3). The high variability in its components: trunks, branches, leaf shapes, heights,

160 densities, fruits and/or seeds, various moisture contents, among others, will have a positive or
161 negative influence on the radar response.

162 The type of dispersion present in broadleaved forests varies (Figure 4). The volumetric dispersion
163 encourages direct backscattering of both the soil, trunk and crown (De Miguel and Gutiérrez
164 2000, Watanabe et al., 2006). If our broad-leaved forest were homogeneous, it is very likely that
165 there are no marked differences between correlations with sparse and dense forests, as was the
166 Espinoza-Mendoza study (2016), but this is not the case. Therefore, it is necessary to consider a
167 distinction in radar response in sparse broadleaf forests and dense broadleaved forests.

168 The double bounce type dispersion could occur in a sparse or very sparse broadleaved forest, due
169 to the existence of voids in the ground with exposed soil. If we consider some of these forests
170 thin as forests in early successional stages, according to Mermoz et al. (2014b) biomass would be
171 overestimated.

172 In dense broadleaved forests, volumetric dispersion will predominate, which will obtain
173 information of all the components present in the middle and lower layers of the canopy, the signal
174 would be attenuated when reaching the ground due to the density of this forest (Joshi et al.,
175 2015a). Linked to this, very dense broadleaved forests are usually mature forests, where the radar
176 signal has a better correspondence than in younger forests (Mermoz et al., 2014a).

177 The diametric groups also fulfill an important factor to achieve a good correlation between the
178 biomass estimated in the field and the backscatter coefficient. For example, the study by Hamdan
179 et al. (2014b) showed that the $DAP > 30$ cm obtained a better correspondence with the radar
180 signal in Malaysian forests. These forests are dominated by dipterocárpeos of low lands, present
181 in areas dedicated to the production of wood with logging activities since the '70s. Espinoza-
182 Mendoza (2016) found that when considering the biomass of individuals > 10 cm, the best
183 correlation was obtained for broadleaf and coniferous forests throughout seven municipalities in

184 the central and northeastern region of Nicaragua, in areas where hypothetically a forest transition
185 would be occurring (Table 2).

186 Through figure 5 we could explain some factors such as the diametric groups: (a) it would
187 represent a very dense broad-leaved forest (without gaps in the ground) that considers tree
188 biomass with $DBH > 10\text{cm}$, with great variability in heights and components. The radar signal in
189 this type of forest would be dispersed volumetrically attenuating as the canopy penetrates towards
190 layers closer to the ground, (b) represents a dense broadleaved forest including biomass of
191 individuals with $DBH > 30\text{cm}$, as in (a) the heights and components have some degree of
192 variability. maintaining a good correlation, (c) represents a broadleaved forest considering only
193 the biomass of individuals with $DBH > 50\text{cm}$, in which not only a volumetric dispersion can be
194 generated, but also a double bounce dispersion. It is observed in table 2 that the correlation
195 decreases significantly. Finally (d) represents a broadleaf forest where only the biomass of trees
196 with $DBH > 70\text{cm}$ is considered, probably high-altitude trees, indicating that there is no
197 correlation with the radar signal (Table 2), and that the signal interacts strongly with the
198 components of middle and lower layers, demonstrating for this case that it is not the larger trees
199 that influence the radar signal.

200

201 **Saturation level**

202 One of the biggest problems with radar images is the saturation of the signal. Ghasemi et al.
203 (2011) consider that the radar signal in complex tropical forests in L and P bands saturates around
204 100 Mg ha^{-1} . Contradictory, Le Toan et al. (2011); Saatchi et al. (2011) and Sandberg et al.
205 (2011) consider that the P band would be saturating from 300 Mg ha^{-1} . In areas considered
206 simple structure and where there are between 1 and 2 species, saturation may occur around 250

207 Mg ha⁻¹. On the other hand, Watanabe et al. (2006) indicate that the saturation level for a single
208 conifer species using the HH polarization was 200 Mg ha⁻¹, whereas if a variety of species
209 (heterogeneous forest) is included, the saturation can vary depending on the polarization: VV =
210 50 tn / ha, HH = 100 tn / ha and HV => 100 tn / ha. As noted, there are different levels of
211 saturation, which will depend to a large extent on the type of polarization used, wavelengths,
212 types and structures of forests and number of species (Figure 6).

213

214 **Masking forest and no forest areas**

215 This factor, although it is true, does not directly influence to the developing model, but, it can
216 have a strong impact when is considered as an external resource. Many areas considered forest
217 may not be so in reality, due to land cover and land use maps are elaborated with different
218 methodologies. Morton et al. (2014) consider that these external resources would cause an impact
219 on the estimated biomass values. Therefore to mitigate to some extent this kind of source of error,
220 we can use a visual review of the plots from which the data were obtained. Supported by tools
221 such as Google Earth, field technical files used at the time of the information gathering of the
222 plots, forest maps and/or high resolution multispectral images that correspond to the dates close
223 to the data collection.

224

225 **Conclusions**

226 1. To estimate biomass in tropical forests using remote radar sensors, the structural characteristics
227 of these should be considered. Because the radar signal, especially the L and P bands act directly
228 with the vegetation components present in these forests.

229 2. Specific equations should be developed for each type of forest. If in a landscape we have:
230 broadleaf forest, coniferous forest, riverside forest and mangrove forest, the best method to obtain
231 good results will be the development of specific models for each type of forest, considering its
232 structural components.

233 3. Generic methodologies, can cause considerable variations in the ABG, by not considering
234 forest parameters related to local areas.

235 4. Generate more information related to the factors that affect the estimation of biomass in
236 tropical forests using remote radar sensors is key to know how the structure of tropical forests,
237 which is highly complex, affects the different bands, polarizations and scattered signals for the
238 components of the forest.

239 5. Analyzing and comparing the multitemporal behavior of the radar signal between tropical
240 forests and agroforestry systems in the tropics, is key to generating information related to forest
241 transitions processes.

242

243

244 **Acknowledgments**

245 Part of some results presented in this research, were obtained in the thesis developed by the
246 author at the Tropical Agronomic Center for Research and Teaching - CATIE to opt for the MSc
247 degree, financed by the World Center for Agroforestry - ICRAF and CATIE, in the country of
248 Nicaragua using data provided by the National Forestry Institute of Nicaragua - INAFOR. For
249 this reason, we thank the institutions mentioned for the academic, financial and technical
250 information provided.

251

252 **Bibliography**

- 253 Avitabile, V., Herold, M., Heuvelink, G., Lewis, S., Phillips, O., Asner, G., Armston, J., Asthon,
254 P., Banin, L., & Bayol, N. (2015). An integrated pan-tropical biomass map using multiple
255 reference datasets. *Global Change Biology*, 22, 1406–1420
- 256 Baccini, A., Goetz, S., Walker, W., Laporte, N., Sun, M., SullaMenashe, D., Hackler, J., Beck, P.,
257 Dubayah, R., & Friedl, M. (2012). Estimated carbon dioxide emissions from tropical
258 deforestation improved by carbon-density maps. *Nature Climate Change*, 2, 182-185
- 259 Baghdadi, N., Le Maire, G., Bailly, J.-S., Osé, K., Nouvellon, Y., Zribi, M., Lemos, C., &
260 Hakamada, R. (2015). Evaluation of ALOS/PALSAR L-band data for the estimation of
261 Eucalyptus plantations aboveground biomass in Brazil. *IEEE Journal of Selected Topics in*
262 *Applied Earth Observations and Remote Sensing*, 8, 3802-3811
- 263 Beaudoin, A., Le Toan, T., Goze, S., Nezry, E., Lopes, A., Mougín, E., Hsu, C., Han, H., Kong,
264 J., & Shin, R. (1994). Retrieval of forest biomass from SAR data. *International Journal of*
265 *Remote Sensing*, 15, 2777-2796
- 266 Behera, M., Tripathi, P., Mishra, B., Kumar, S., Chitale, V., & Behera, S.K. (2016). Above-
267 ground biomass and carbon estimates of *Shorea robusta* and *Tectona grandis* forests using
268 QuadPOL ALOS PALSAR data. *Advances in Space Research*, 57, 552-561
- 269 Brown, S. (1997). *Estimating biomass and biomass change of tropical forests*. (134 ed.). Roma,
270 Italia: Food & Agriculture Org.
- 271 Collins, J., Hutley, L.B., Williams, R., Boggs, G., Bell, D., & Bartolo, R. (2009). Estimating
272 landscape-scale vegetation carbon stocks using airborne multi-frequency polarimetric
273 synthetic aperture radar (SAR) in the savannahs of north Australia. *International Journal of*
274 *Remote Sensing*, 30, 1141-1159

- 275 Chave, J., Andalo, C., Brown, S., Cairns, M., Chambers, J., Eamus, D., Fölster, H., Fromard, F.,
276 Higuchi, N., & Kira, T. (2005). Tree allometry and improved estimation of carbon stocks and
277 balance in tropical forests. *Oecologia*, 145, 87-99
- 278 Chave, J., Réjou-Méchain, M., Búrquez, A., Chidumayo, E., Colgan, M.S., Delitti, W.B., Duque,
279 A., Eid, T., Fearnside, P.M., & Goodman, R.C. (2014a). Improved allometric models to
280 estimate the aboveground biomass of tropical trees. *Global Change Biology*, 20, 3177-3190
- 281 Chave, J., Réjou-Méchain, M., Búrquez, A., Chidumayo, E., Colgan, M.S., Delitti, W.B.C.,
282 Duque, A., Eid, T., Fearnside, P.M., & Goodman, R.C. (2014b). Improved allometric models
283 to estimate the aboveground biomass of tropical trees. *Global Change Biology*, 20, 3177-3190
- 284 Chave, J., Riéra, B., & Dubois, M.-A. (2001). Estimation of biomass in a neotropical forest of
285 French Guiana: spatial and temporal variability. *Journal of Tropical Ecology*, 17, 79-96
- 286 De Miguel, S.M., & Gutiérrez, J.S. (2000). Estimación de biomasa en masas regulares por medio
287 de imágenes de radar. In, *Ciencia y tecnología de la información geográfica en un mundo*
288 *globalizado: X Congreso del Grupo de Métodos Cuantitativos, Sistemas de Información*
289 *Geográfica y Teledetección* (p. 47)
- 290 Dobson, M.C., Ulaby, F.T., LeToan, T., Beaudoin, A., Kasischke, E.S., & Christensen, N.
291 (1992). Dependence of radar backscatter on coniferous forest biomass. *IEEE Transactions on*
292 *Geoscience and Remote Sensing*, 30, 412-415
- 293 Drake, J.B., Knox, R.G., Dubayah, R.O., Clark, D.B., Condit, R., Blair, J.B., & Hofton, M.
294 (2003). Above-ground biomass estimation in closed canopy neotropical forests using lidar
295 remote sensing: factors affecting the generality of relationships. *Global Ecology and*
296 *Biogeography*, 12, 147-159
- 297 Espinoza-Mendoza, V.E. (2016). Impulsores de cambio en el uso de suelo y almacenamiento de
298 carbono sobre un gradiente de modificación humana de Paisajes en Nicaragua. In (p. 170).

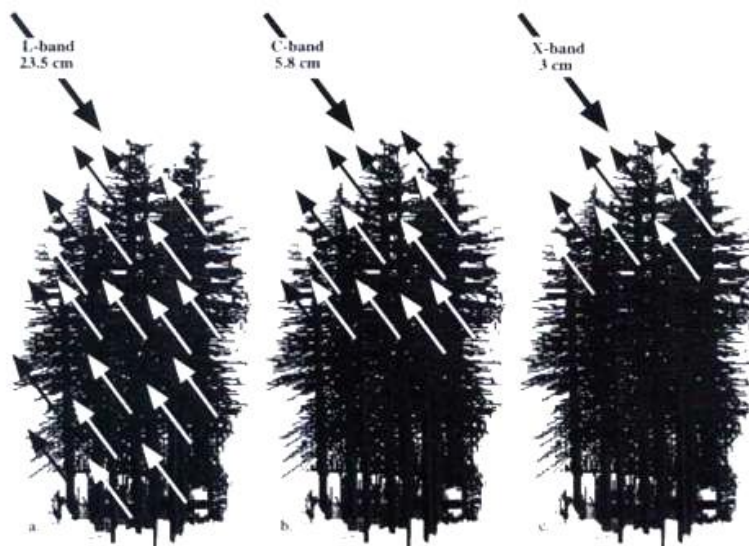
- 299 Turrialba, Costa Rica: CATIE
- 300 Feldpausch, T.R., McDonald, A.J., Passos, C.A., Lehmann, J., & Riha, S.J. (2006). Biomass,
301 harvestable area, and forest structure estimated from commercial timber inventories and
302 remotely sensed imagery in southern Amazonia. *Forest Ecology and Management*, 233, 121-
303 132
- 304 Ghasemi, N., Sahebi, M.R., & Mohammadzadeh, A. (2011). A review on biomass estimation
305 methods using synthetic aperture radar data. *International Journal of Geomatics and*
306 *Geosciences*, 1, 776-788
- 307 Goetz, S.J., Baccini, A., Laporte, N.T., Johns, T., Walker, W., Kellndorfer, J., Houghton, R.A., &
308 Sun, M. (2009). Mapping and monitoring carbon stocks with satellite observations: a
309 comparison of methods. *Carbon Balance and Management*, 4, 2
- 310 Hamdan, O., Aziz, H.K., & Rahman, K.A. (2011). Remotely sensed L-Band SAR data for
311 tropical forest biomass estimation. *Journal of Tropical Forest Science*, 23, 318-327
- 312 Hamdan, O., Khali Aziz, H., & Mohd Hasmadi, I. (2014a). L-band ALOS PALSAR for biomass
313 estimation of Matang Mangroves, Malaysia. *Remote Sensing of Environment*, 155, 69-78
- 314 Hamdan, O., Mohd Hasmadi, I., HKhali Aziz, H., Norizah, K., & Hlmi Zuhaidi, M.S. (2014b).
315 Factors Affecting L-Band Alos Palsar Backscatter on Tropical Forest Biomass. *Global Journal*
316 *of Science Frontier Research*, 14, 51-63
- 317 Hensley, S., Oveisgharan, S., Saatchi, S., Simard, M., Ahmed, R., & Haddad, Z. (2014). An error
318 model for biomass estimates derived from polarimetric radar backscatter. *IEEE Transactions*
319 *on Geoscience and Remote Sensing*, 52, 4065-4082
- 320 Holdridge, L.R., & Grenke, W.C. (1971). Forest environments in tropical life zones: a pilot study.
321 Forest environments in tropical life zones: a pilot study.

- 322 Imhoff, M. (1995). Radar backscatter and biomass saturation: ramifications for global biomass
323 inventory. *IEEE Transactions on Geoscience and Remote Sensing*, 33, 511-518.
- 324 Joshi, N.P., Mitchard, E.T., Schumacher, J., Johannsen, V.K., Saatchi, S., & Fensholt, R. (2015a).
325 L-Band SAR Backscatter Related to Forest Cover, Height and Aboveground Biomass at
326 Multiple Spatial Scales across Denmark. *Remote Sensing*, 7, 4442- 4472
- 327 Joshi, N.P., Mitchard, E.T.A., Schumacher, J., Johannsen, V.K., Saatchi, S., & Fensholt, R.
328 (2015b). L-band SAR backscatter related to forest cover, height and aboveground biomass at
329 multiple spatial scales across Denmark. *Remote Sensing*, 7, 4442- 4472
- 330 Kato, R., Tadaki, Y., & Ogawa, H. (1978). Plant biomass and growth increment studies in Pasoh
331 Forest. *Malayan Nature Journal*
- 332 Keller, M., Palace, M., & Hurtt, G. (2001). Biomass estimation in the Tapajos National Forest,
333 Brazil: examination of sampling and allometric uncertainties. *Forest Ecology and*
334 *Management*, 154, 371-382
- 335 Ketterings, Q.M., Coe, R., van Noordwijk, M., & Palm, C.A. (2001). Reducing uncertainty in the
336 use of allometric biomass equations for predicting above-ground tree biomass in mixed
337 secondary forests. *Forest Ecology and Management*, 146, 199-209
- 338 Koch, B. (2013). Remote Sensing supporting national forest inventories NFA. *FAO knowledge*
339 *reference for national forest assessments*, 15
- 340 Le Toan, T., Beaudoin, A., Riom, J., & Guyon, D. (1992). Relating forest biomass to SAR data.
341 *Geoscience and Remote Sensing, IEEE Transactions on*, 30, 403-411
- 342 Le Toan, T., Quegan, S., Davidson, M., Balzter, H., Paillou, P., Papathanassiou, K., Plummer, S.,
343 Rocca, F., Saatchi, S., & Shugart, H. (2011). The BIOMASS mission: Mapping global forest
344 biomass to better understand the terrestrial carbon cycle. *Remote Sensing of Environment*,
345 115, 2850-2860

- 346 Louman, B. (2001). *Silvicultura de bosques latifoliados húmedos con énfasis en América Central.*
347 CATIE
- 348 Luckman, A., Baker, J., Kuplich, T.M., Yanasse, C.d.C.F., & Frery, A.C. (1997). A study of the
349 relationship between radar backscatter and regenerating tropical forest biomass for spaceborne
350 SAR instruments. *Remote Sensing of Environment*, 60, 1-13
- 351 Mermoz, S., Le Toan, T., Villard, L., Réjou-Méchain, M., & SeifertGranzin, J. (2014a). Biomass
352 assessment in the Cameroon savanna using Alos Palsar data. *Remote Sensing of Environment*,
353 155, 109-119
- 354 Mermoz, S., Rejou-Mechain, M., Villard, L., Le Toan, T., Rossi, V., & Gourlet-Fleury, S.
355 (2014b). Biomass of dense forests related to L-band SAR backscatter? In, *Geoscience and*
356 *Remote Sensing Symposium (IGARSS), 2014 IEEE International* (pp. 1037-1040)
- 357 Michelakis, Stuart, Brolly, Lopez, & Linares. (2015). Estimation of Woody Biomass of Pine
358 Savanna Woodlands from Alos Palsar Imagery. *Journal of selected topics in applied earth*
359 *observations and remote sensing*, 8, 244-254
- 360 Mitchard, E., Saatchi, S., Gerard, F., Lewis, S., & Meir, P. (2009). Measuring woody
361 encroachment along a forest-savanna boundary in Central Africa. *Earth Interactions*, 13, 1-29
- 362 Mitchard, E.T., Meir, P., Ryan, C.M., Woollen, E.S., Williams, M., Goodman, L.E., Mucavele,
363 J.A., Watts, P., Woodhouse, I.H., & Saatchi, S.S. (2013). A novel application of satellite radar
364 data: measuring carbon sequestration and detecting degradation in a community forestry
365 project in Mozambique. *Plant Ecology & Diversity*, 6, 159-170
- 366 Morton, D.C., Nagol, J., Carabajal, C.C., Rosette, J., Palace, M., Cook, B.D., Vermote, E.F.,
367 Harding, D.J., & North, P.R. (2014). Amazon forests maintain consistent canopy structure and
368 greenness during the dry season. *Nature*, 506, 221-224

- 369 Pearson, T., Walker, S., & Brown, S. (2005). Sourcebook for land use, land-use change and
370 forestry projects. Winrock International.
- 371 Pulliainen, J., Kurvonen, L., and Hallikainen, M. T. (1999). Multitemporal behavior of L-and C-
372 band SAR observations of boreal forests. *IEEE Transactions on Geoscience and Remote*
373 *Sensing*, 37(2), 927-937.
- 374 Quijano, A. & Morales, Y. (2016). Modelo regresivo para la estimación de biomasa aérea forestal
375 a partir de datos de parcelas permanentes y datos Radar SAR ALOS PALSAR en el Parque
376 Natural Bataclán, Cali. *UD y la Geomática*, 11, 66-72.
- 377 Saatchi, S.S., Harris, N.L., Brown, S., Lefsky, M., Mitchard, E.T., Salas, W., Zutta, B.R.,
378 Buermann, W., Lewis, S.L., & Hagen, S. (2011). Benchmark map of forest carbon stocks in
379 tropical regions across three continents. In, *Proceedings of the National Academy of Sciences*
380 (pp. 9899-9904)
- 381 Sandberg, G., Ulander, L.M., Fransson, J., Holmgren, J., & Le Toan, T. (2011). L-and P-band
382 backscatter intensity for biomass retrieval in hemiboreal forest. *Remote Sensing of*
383 *Environment*, 115, 2874-2886
- 384 Sinha, S., Jeganathan, C., Sharma, L., & Nathawat, M. (2015). A review of radar remote sensing
385 for biomass estimation. *International Journal of Environmental Science and Technology*, 12,
386 1779-1792
- 387 Sola, G., Picard, N., Saint-André, L., & Henry, M. (2012). Resumen del manual de construcción
388 de ecuaciones alométricas para estimar el volumen y la biomasa de los árboles: del trabajo de
389 campo a la predicción. Roma, Montpellier: Las Naciones Unidas para la Alimentación y la
390 Agricultura y el Centre de Coopération Internationale en Recherche Agronomique pour le
391 Développement

- 392 Thumaty, K.C., Fararoda, R., Middinti, S., Gopalakrishnan, R., Jha, C.S., & Dadhwal, V.K.
393 (2016). Estimation of Above Ground Biomass for Central Indian Deciduous Forests Using
394 ALOS PALSAR L-Band Data. *Journal of the Indian Society of Remote Sensing*, 44, 31-39
- 395 Van Zyl, J.J. (1993). The effect of topography on radar scattering from vegetated areas.
396 *Geoscience and Remote Sensing*, 31, 153- 160
- 397 Walker, W., A. Baccini, M. Nepstad, N. Horning, D. Knight, E. Braun, y A. Bausch. (2011).
398 Guía de Campo para la Estimación de Biomasa y Carbono Forestal. Versión 1.0. Falmouth,
399 Massachusetts, USA.: Woods Hole Research Center
- 400 Wang, Y., Davis, F., Melack, J., Kasischke, E., & Christensen Jr, N. (1995). The effects of
401 changes in forest biomass on radar backscatter from tree canopies. *Remote Sensing*, 16, 503-
402 513
- 403 Watanabe, M., Shimada, M., Rosenqvist, A., Tadono, T., Matsuoka, M., Romshoo, S.A., Ohta,
404 K., Furuta, R., Nakamura, K., & Moriyama, T. (2006). Forest Structure Dependency of the
405 Relation Between L-Band and Biophysical Parameters. *IEEE Transactions on Geoscience and*
406 *Remote Sensing*, 44, 3154-3165
- 407 Woodhouse, I.H., Mitchard, E.T., Brolly, M., Maniatis, D., & Ryan, C.M. (2012). Radar
408 backscatter is not a direct measure of forest biomass. *Nature Climate Change*, 2, 556-557
- 409 Yu, Y., & Saatchi, S. (2016). Sensitivity of L-Band SAR Backscatter to Aboveground Biomass
410 of Global Forests. *Remote Sensing*, 8, 522.
- 411



412

413

414 **Figure 1:** Wavelengths. The arrows indicate the penetration capacity of the X, C and L bands
415 through the canopy (Jensen 2000).

416

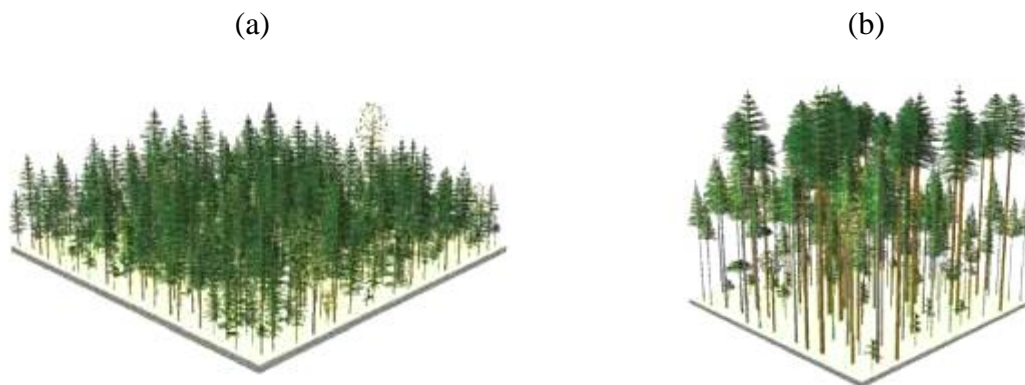
417 **Table 1:** Diversity of allometric equations to be considered for the estimation of biomass using
418 data taken in the field (Own elaboration).

419

Referencia	Modelo alométrico
Chave et al. (2005)	$\rho X \exp(\alpha + \beta_1 \ln(DAP)) + \beta_2 (\ln(DAP))^2 - \beta_3 (\ln(DAP))^3$
Chave et al. (2014a)	$\ln(AGB) = \alpha + \beta \ln(\rho * D^2 * H) + \varepsilon$
Brown (1997) Seco pp=900-1500mm	$B = 0.2035 * DAP^{2.3196}$
Brown (1997) Húmedo pp=1500-4000mm	$B = \exp(-2.289 + 2.649 * \ln(DAP) - 0.021 * \ln(DAP^2))$
Brown (1997) Muy Húmedo (pp > 4000mm)	$B = 21.297 - 6.953 * DAP + 0.740 * DAP^2$
Chambers et al.(2001)	$B = \exp(\alpha + \beta_1 \ln(DAP) + \beta_2 (\ln(DAP))^2 - \beta_3 (\ln(DAP))^3)$
Burger (2005)	$B = \exp(\alpha + \beta_1 \ln(Dbase))$
Tiepolo et al. (2002)	$B = \alpha + \beta_1 (DAP) + \beta_2 (DAP)^2$
Feldspausch (2012)	$B = \exp(a + b \ln(DAP) + c (\ln(DAP))^2 - d (\ln(DAP))^3 + e \ln(\rho w))$

420

421



422

423 **Figure 2:** Sketch of mature coniferous forests. A dense and homogeneous (a) profile is observed,

424 representing a coniferous forest in which a specie predominates. While (b) shows a forest of

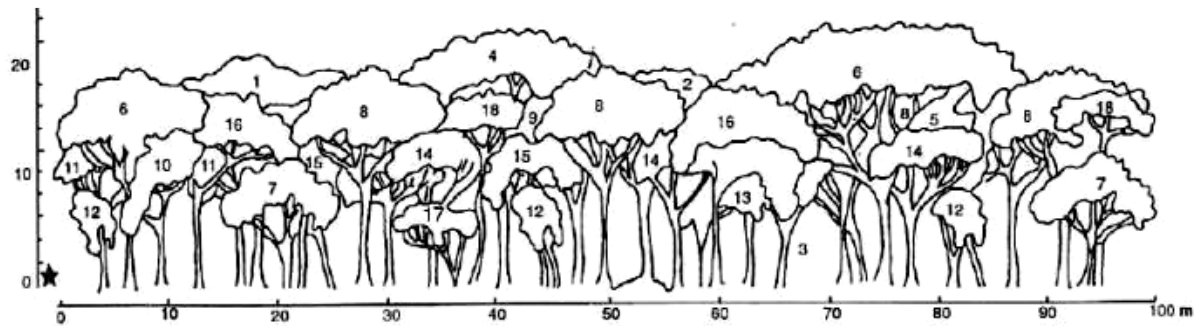
425 conifers with multiple strata, with different stages of growth, less dense than (a), with greater

426 variability in heights and where 2 or 3 species of pine would predominate. Even so, it is observed

427 that their structures have a greater homogeneity than a broadleaved forest.

428

429

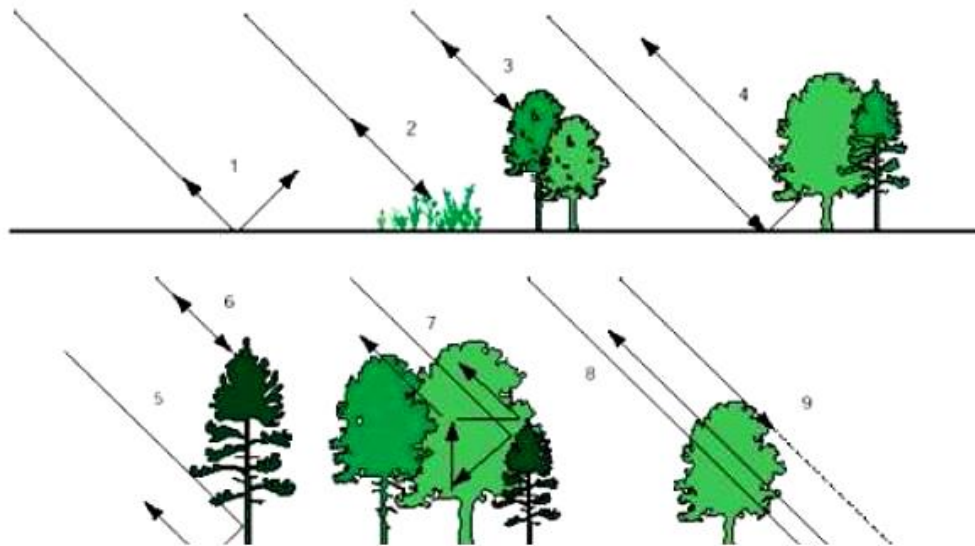


430

431

432 **Figure 3:** Louman (2001). The scheme shows the idealized profile of a wet forest premontane
 433 transition to tropical (Holdridge and Grenke 1971). There is a variety of heights, trunk forms,
 434 canopy, branches and each number represent a different species.

435



436

437

438 **Figure 4:** Different types of dispersion present in a forest (Piowar, 1997) (1) Diffuse dispersion
 439 from the surface (2) and (3) Direct dispersion of various components of the vegetation (4) Double
 440 dispersion rebound of the soil interaction - vegetation (5) Corner reflection between trunk and
 441 surface (6) Direct backscattering of the upper layer of the canopy (7) Volumetric dispersion from

21

442 within the canopy (8) Diffuse dispersion from the surface (9) Shadows caused by parts of the
 443 forest canopy or other parts of the canopy and / or the surface.

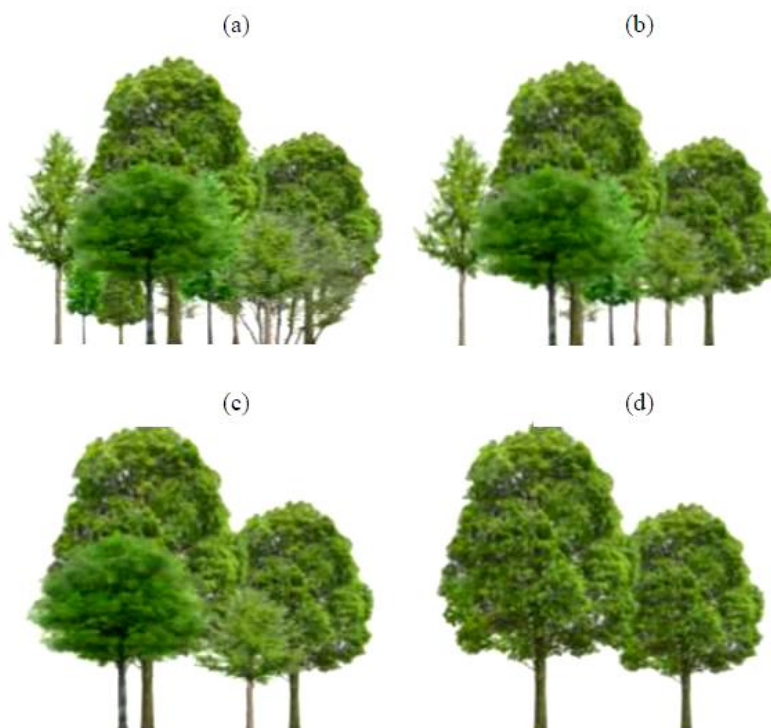
444

445 **Table 2:** Correlations between the biomass present in different diametric groups and the radar
 446 signal (Espinoza-Mendoza 2016).

DAP	Pearson	# de parcelas
≥10cm	0.74(p<0.0001)	74
>20cm	0.73(p<0.0001)	72
>30cm	0.67(p<0.0001)	65
≥40cm	0.57(p<0.0001)	53
≥50cm	0.50(p<0.0001)	46
>60cm	0.34(p<0.1100)	34
>70cm	0.13(p<0.5351)	26

447

448

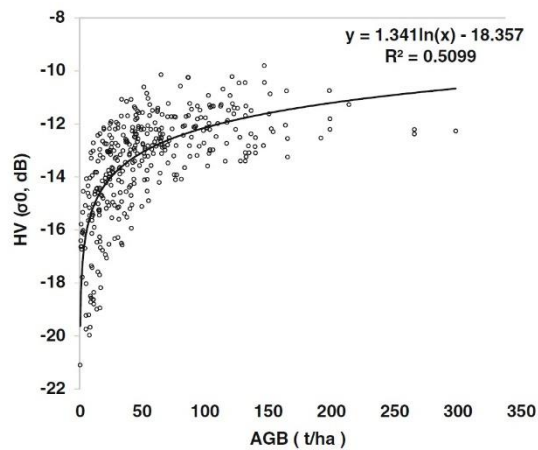
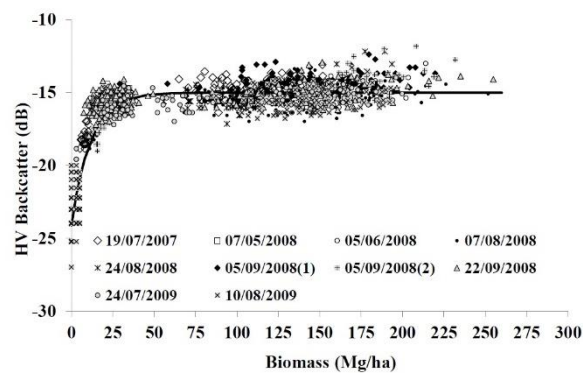


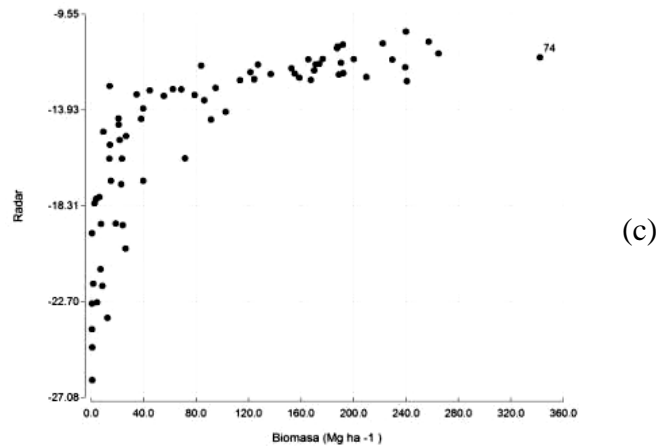
449

450 **Figure 5:** Forest structure and biomass (Espinoza-Mendoza 2016).

451

452
453
454
455
456
457
458
459
460
461





462

463 **Figure 6:** Different levels of saturation. Biomass estimated in field vs HV. a: Baghdadi et al.
464 (2015) around 60 Mg ha⁻¹ in eucalyptus plantations in Brazil in HV polarization; b: Thumaty et
465 al. (2016), greater than 150 Mg ha⁻¹ in HV polarization in deciduous forests in India; c:
466 Espinoza-Mendoza (2016), around 130 Mg ha⁻¹ in Nicaraguan forests.

467